

Electronic supplementary information – First-principles study on  
structural, electronic and optical properties of halide double perovskite  
 $\text{Cs}_2\text{AgBX}_6$  ( $\text{B} = \text{In}, \text{Sb}$ ;  $\text{X} = \text{F}, \text{Cl}, \text{Br}, \text{I}$ )

Chol-Jun Yu\*, Il-Chol Ri, Hak-Myong Ri, Jong-Hyok Jang, Yun-Sim Kim and Un-Gi Jong

*Computational Materials Design, Faculty of Materials Science, Kim Il Sung University,  
Pyongyang, PO Box 76, Democratic People's Republic of Korea*

Table S1. Total energy ( $E_{\text{tot}}$ ) and total energy per formula unit (fu) of elementary and binary solids with crystalline phase and space group.

Solid	Phase	Space group	Ref.	$E_{\text{tot}}$ (Ry)	$E_{\text{tot}}$ per fu (Ry)
Cs	fcc	$Fm\bar{3}m$	[1]	-252.261140	-63.065285
	bcc	$I\bar{m}\bar{3}m$	[1]	-126.130728	-63.065364
Ag	fcc	$Fm\bar{3}m$	[2]	-1182.487992	-295.621998
In	tetragonal	$I4/M\bar{M}M$	[3]	-266.963872	-133.481936
	orthorhombic	$Fmmm$	[4]	-533.916447	-133.479112
Sb	fcc	$Fm\bar{3}m$	[5]	-739.705388	-184.926347
	tetragonal	$I4/M\bar{M}M$	[5]	-369.909949	-184.954974
	hexagonal	$R\bar{3}mh$	[6]	-1109.711095	-184.951849
AgF	cubic	$Fm\bar{3}m$		-1376.882710	-344.220678
AgCl	cubic	$Fm\bar{3}m$	[7]	-1315.916179	-328.979045
AgBr	cubic	$Fm\bar{3}m$	[8]	-1370.075394	-342.518849
AgI	cubic	$Fm\bar{3}m$	[9]	-1445.211938	-361.302985
	hexagonal	$P6\bar{3}mc$	[10]	-722.632490	-361.316245
	zinc blonde	$F\bar{4}3m$	[9]	-1445.267447	-361.316862
CsF	cubic	$Fm\bar{3}m$	[12]	-447.652490	-111.913122
	cubic	$Pm\bar{3}m$	[11]	-111.897148	-111.897148
CsCl	cubic	$Fm\bar{3}m$	[12]	-386.585878	-96.646470
	cubic	$Pm\bar{3}m$	[11]	-96.641591	-96.641591
CsBr	cubic	$Fm\bar{3}m$	[12]	-440.706264	-110.176566
	cubic	$Pm\bar{3}m$	[11]	-110.172869	-110.172869
CsI	cubic	$Fm\bar{3}m$	[12]	-515.767250	-128.941813
	cubic	$Pn\bar{3}m$	[11]	-128.940813	-128.940813
$\text{InF}_3$	monoclinic	$C12/m1$	[13]	-1118.322334	
$\text{InCl}_3$	monoclinic	$C12/m1$		-934.731573	
$\text{InBr}_3$	monoclinic	$C12/m1$		-1097.071959	
$\text{InI}_3$	monoclinic	$P121/c1$	[14]	-1322.317962	
$\text{SbF}_3$	orthorhombic	$Pnma$	[15]	-1324.036195	
$\text{SbCl}_3$	orthorhombic	$Pnma$		-1140.329477	
$\text{SbBr}_3$	orthorhombic	$Pbnm$		-1302.674655	
$\text{SbI}_3$	monoclinic	$P121/c1$		-1527.973965	

\*Corresponding author: Chol-Jun Yu, Email: cj.yu@ryongnamsan.edu.kp

Table S2. Total energy ( $E_{\text{tot}}$ ) of halide double perovskites  $\text{CsAgBX}_6$  (B = In, Sb; X = F, Cl, Br, I) and elementary substances of Cs, Ag, In, Sb and  $\text{X}_2$ , and the elementary formation energy ( $E_f$ ) per formula unit (fu).

Compound	$E_{\text{tot}}$ (Ry)	$E_{\text{tot}}$ (Ry)				$\Delta E$ (Ry)	$E_f$ (eV/fu)
		Cs	Ag	In/Sb	$\text{X}_2$		
$\text{Cs}_2\text{AgInF}_6$	-847.752926	-126.130728	-1182.487992	-266.963872	-96.918306	-1.7633	-23.9915
$\text{Cs}_2\text{AgInCl}_6$	-756.016824	-126.130728	-1182.487992	-266.963872	-66.573755	-1.0609	-14.4342
$\text{Cs}_2\text{AgInBr}_6$	-837.175734	-126.130728	-1182.487992	-266.963872	-93.671579	-0.9263	-12.6034
$\text{Cs}_2\text{AgInI}_6$	-949.782210	-126.130728	-1182.487992	-266.963872	-131.271802	-0.7321	-9.9613
$\text{Cs}_2\text{AgSbF}_6$	-899.126947	-126.130728	-1182.487992	-369.909949	-96.918306	-1.6643	-22.6443
$\text{Cs}_2\text{AgSbCl}_6$	-807.416302	-126.130728	-1182.487992	-369.909949	-66.573755	-0.9873	-13.4334
$\text{Cs}_2\text{AgSbBr}_6$	-888.595342	-126.130728	-1182.487992	-369.909949	-93.671579	-0.8729	-11.8764
$\text{Cs}_2\text{AgSbI}_6$	-1001.224795	-126.130728	-1182.487992	-369.909949	-131.271802	-0.7017	-9.5469

Table S3. Total energy ( $E_{\text{tot}}$ ) of halide double perovskites  $\text{CsAgBX}_6$  and the binary compounds of  $\text{CsX}$ ,  $\text{AgX}$  and  $\text{BX}_3$ , and the binary formation energy ( $E_f$ ) per formula unit (fu).

Compound	$E_{\text{tot}}$ (Ry)	$E_{\text{tot}}$ (Ry)			$\Delta E$ (Ry)	$E_f$ (eV/fu)
		CsX	AgX	$\text{BX}_3$		
$\text{Cs}_2\text{AgInF}_6$	-847.752926	-447.652490	-1376.882710	-1118.322334	-0.1254	-1.7064
$\text{Cs}_2\text{AgInCl}_6$	-756.016824	-386.585878	-1315.916179	-934.731573	-0.0619	-0.8428
$\text{Cs}_2\text{AgInBr}_6$	-837.175734	-440.706264	-1370.075394	-1097.071959	-0.0358	-0.4866
$\text{Cs}_2\text{AgInI}_6$	-949.782210	-515.767250	-1445.267447	-1322.317962	-0.0022	-0.0304
$\text{Cs}_2\text{AgSbF}_6$	-899.126947	-447.652490	-1376.882710	-1324.036195	-0.0710	-0.9657
$\text{Cs}_2\text{AgSbCl}_6$	-807.416302	-386.585878	-1315.916179	-1140.329477	-0.0619	-0.8429
$\text{Cs}_2\text{AgSbBr}_6$	-888.595342	-440.706264	-1370.075394	-1302.674655	-0.0547	-0.7442
$\text{Cs}_2\text{AgSbI}_6$	-1001.224795	-515.767250	-1445.267447	-1527.990350	-0.0267	-0.3636

Table S4. Effective mass of electron ( $m_e$ ) and hole ( $m_h$ ) in the three Cartesian directions ( $x$ ,  $y$ ,  $z$ ), and their harmonic mean values calculated by  $m^* = 3/(1/m_x + 1/m_y + 1/m_z)$ .

Compound	$m_e$				$m_h$			
	$x$	$y$	$z$	$m^*$	$x$	$y$	$z$	$m^*$
$\text{Cs}_2\text{AgInF}_6$	0.4090	0.4090	0.4090	0.4090	1.1829	1.1829	1.7791	1.3317
$\text{Cs}_2\text{AgInCl}_6$	0.2716	0.2716	0.2716	0.2716	0.4626	0.4626	0.6030	0.5015
$\text{Cs}_2\text{AgInBr}_6$	0.1614	0.1614	0.1614	0.1614	0.3392	0.3392	0.5077	0.3814
$\text{Cs}_2\text{AgInI}_6$	0.1062	0.1062	0.1062	0.1062	0.2433	0.2433	0.4212	0.2832
$\text{Cs}_2\text{AgSbF}_6$	0.6062	0.5826	0.5769	0.5883	0.5974	1.0447	0.7601	0.7601
$\text{Cs}_2\text{AgSbCl}_6$	0.3646	0.3511	0.3479	0.3544	0.3382	0.5879	0.4294	0.4294
$\text{Cs}_2\text{AgSbBr}_6$	0.2803	0.2659	0.2625	0.2693	0.2911	0.5181	0.3728	0.3728
$\text{Cs}_2\text{AgSbI}_6$	0.2088	0.1895	0.1852	0.1940	0.2536	0.4508	0.3246	0.3246

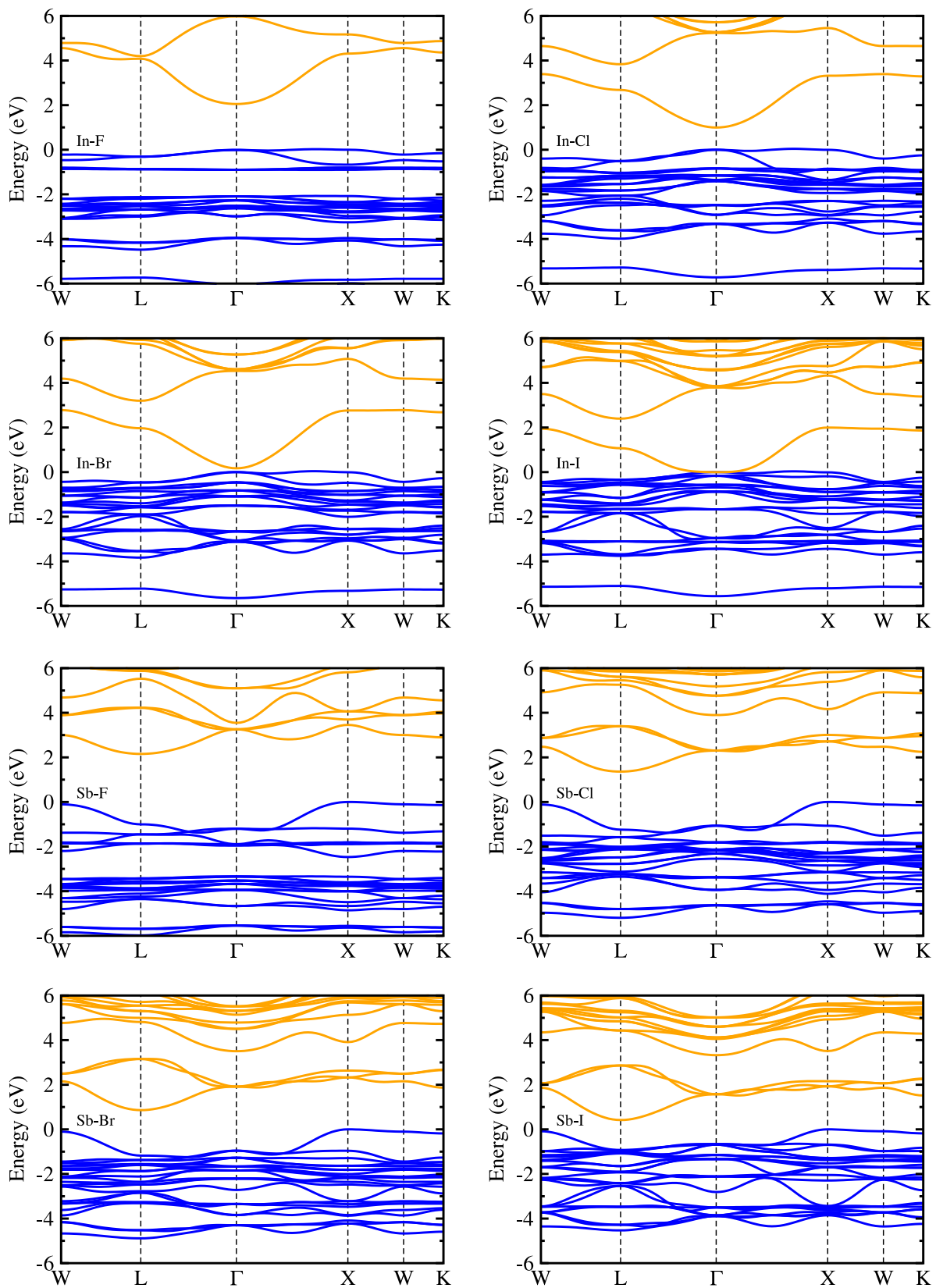


Figure S1. Electronic band structures of all-inorganic halide double perovskites  $\text{Cs}_2\text{Ag}\text{BX}_6$  ( $\text{B} = \text{In}, \text{Sb}$ ;  $\text{X} = \text{F}, \text{Cl}, \text{Br}, \text{I}$ ), calculated with PBE functional.

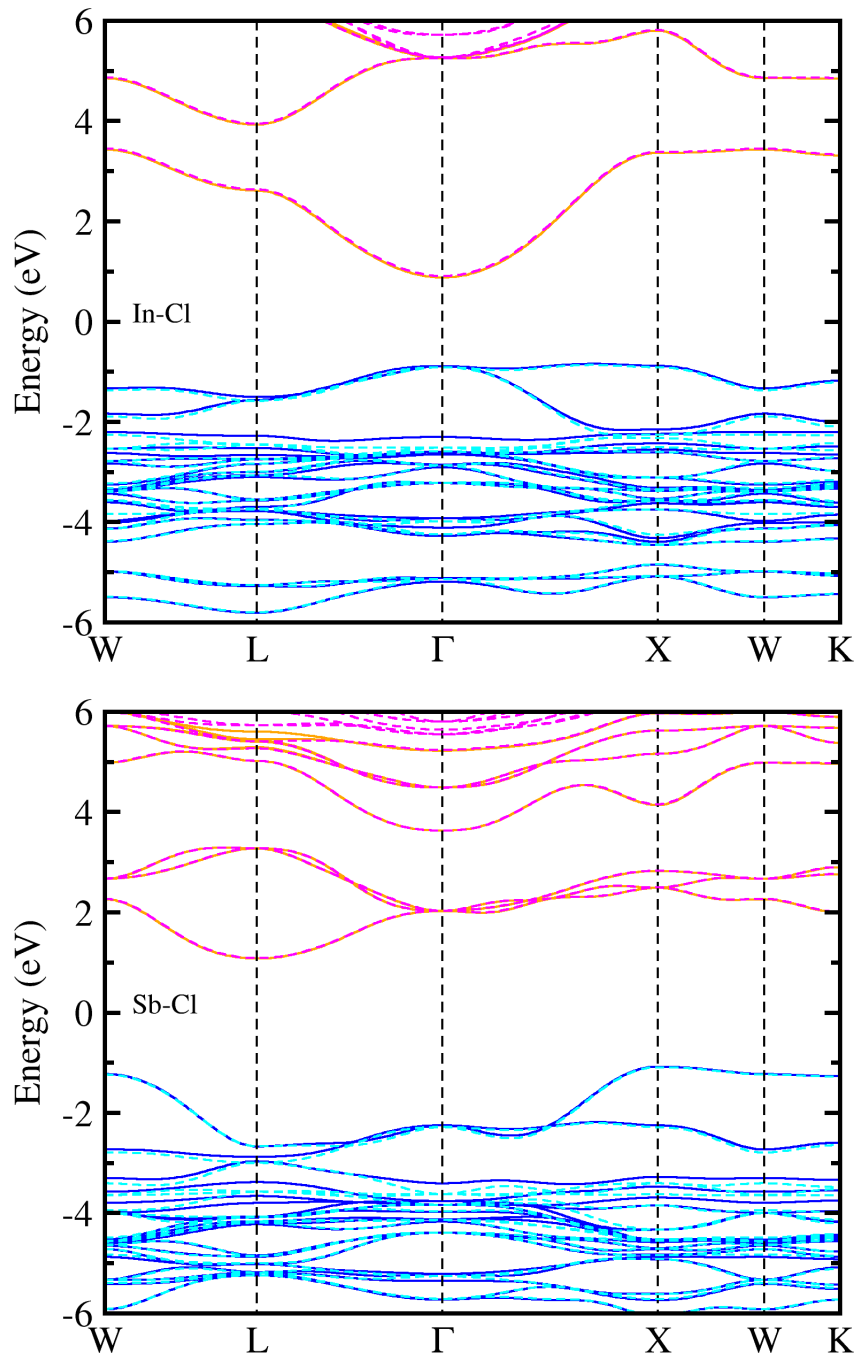


Figure S2. Electronic band structures of all-inorganic halide double perovskites  $\text{Cs}_2\text{AgInCl}_6$  (top) and  $\text{Cs}_2\text{AgSbCl}_6$  (bottom), calculated with PBE (solid lines) and PBE+SOC (dashed lines).

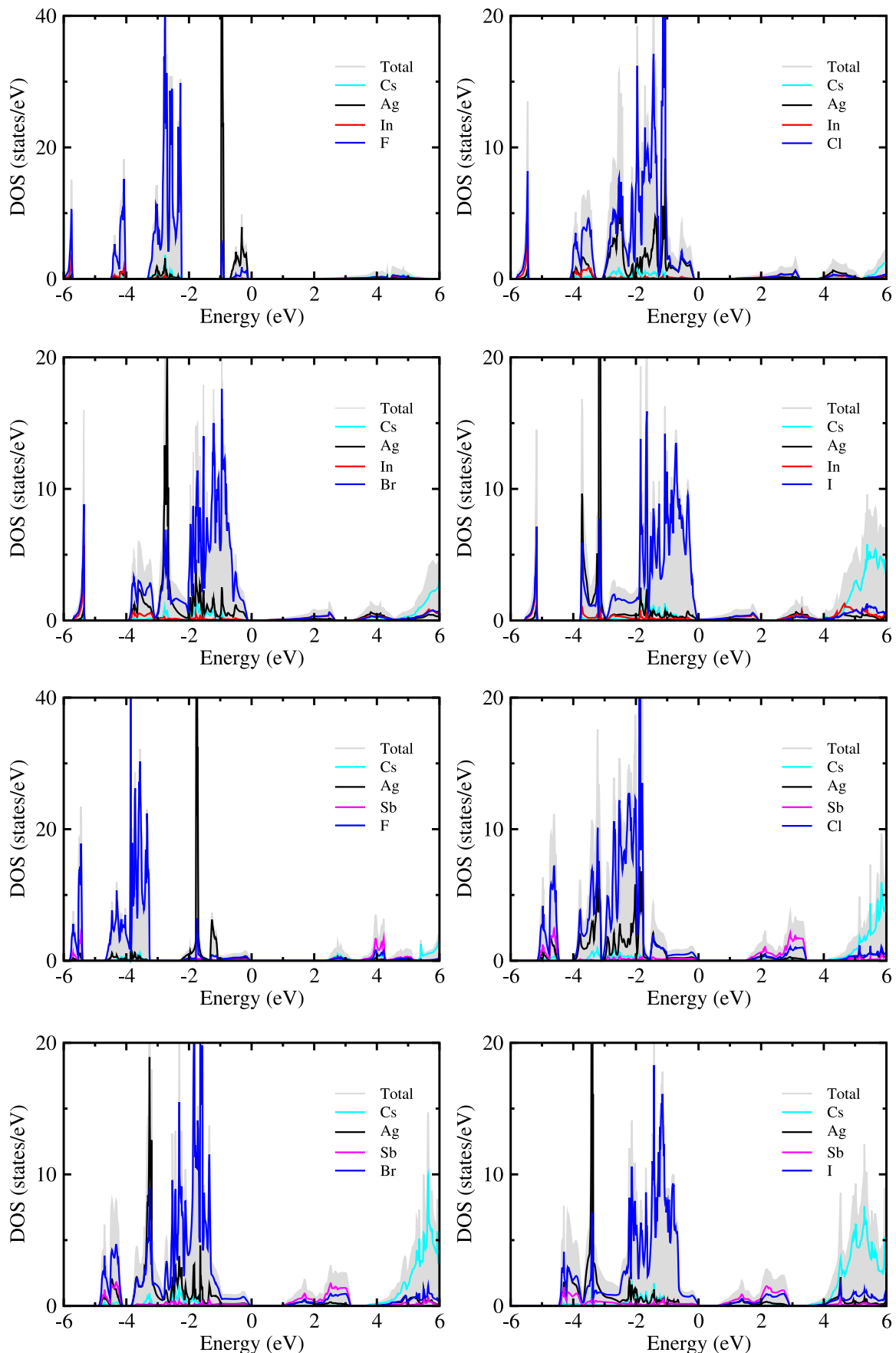


Figure S3. Atom-projected total density of states (DOS) of all-inorganic halide double perovskites  $\text{Cs}_2\text{AgBX}_6$  ( $\text{B} = \text{In}, \text{Sb}$ ;  $\text{X} = \text{F}, \text{Cl}, \text{Br}, \text{I}$ ), calculated with HSE hybrid functional.

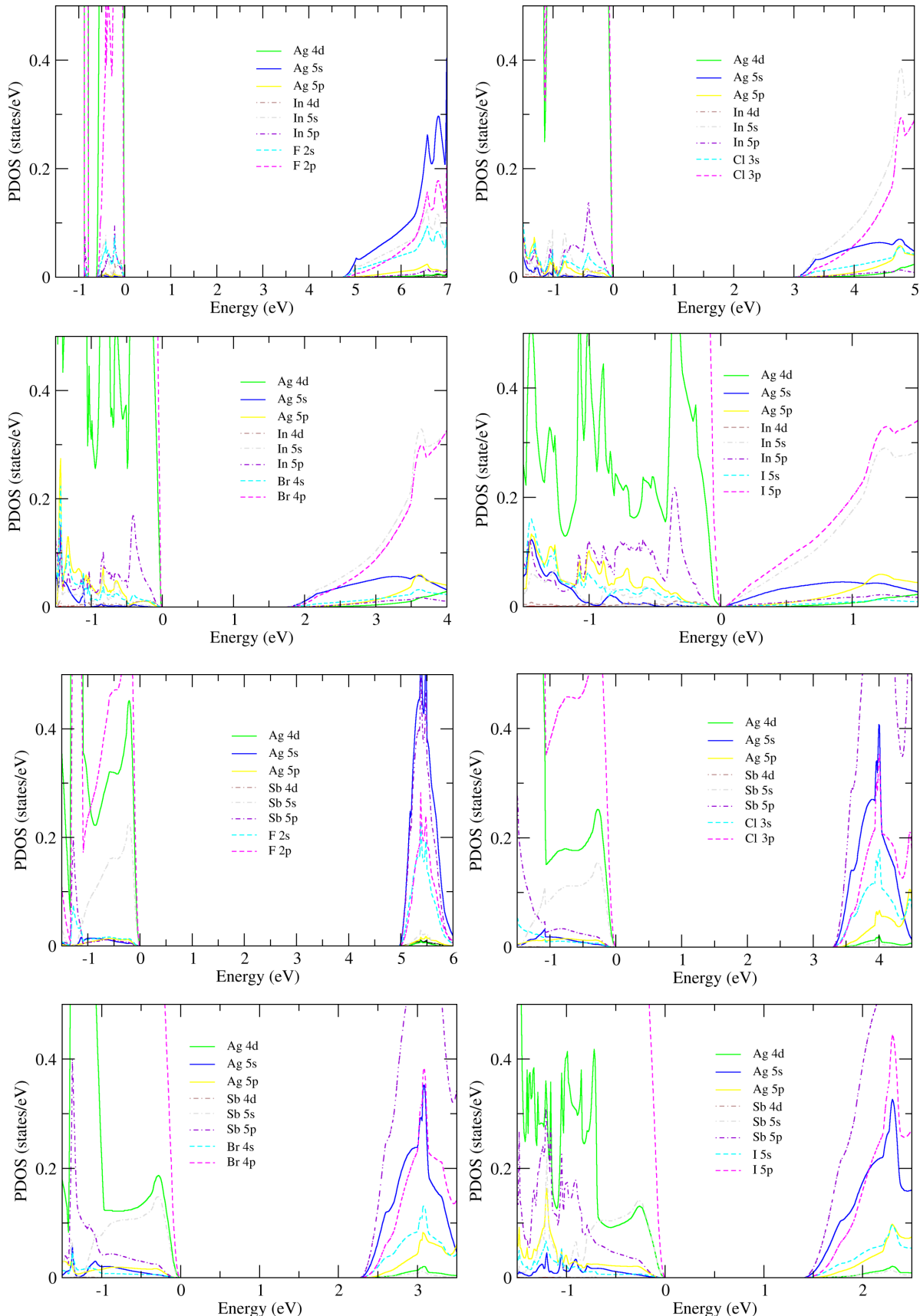


Figure S4. Orbital-resolved partial density of states (PDOS) of all-inorganic halide double perovskites  $\text{Cs}_2\text{AgBX}_6$  ( $\text{B} = \text{In}, \text{Sb}; \text{X} = \text{F}, \text{Cl}, \text{Br}, \text{I}$ ), calculated with HSE hybrid functional.

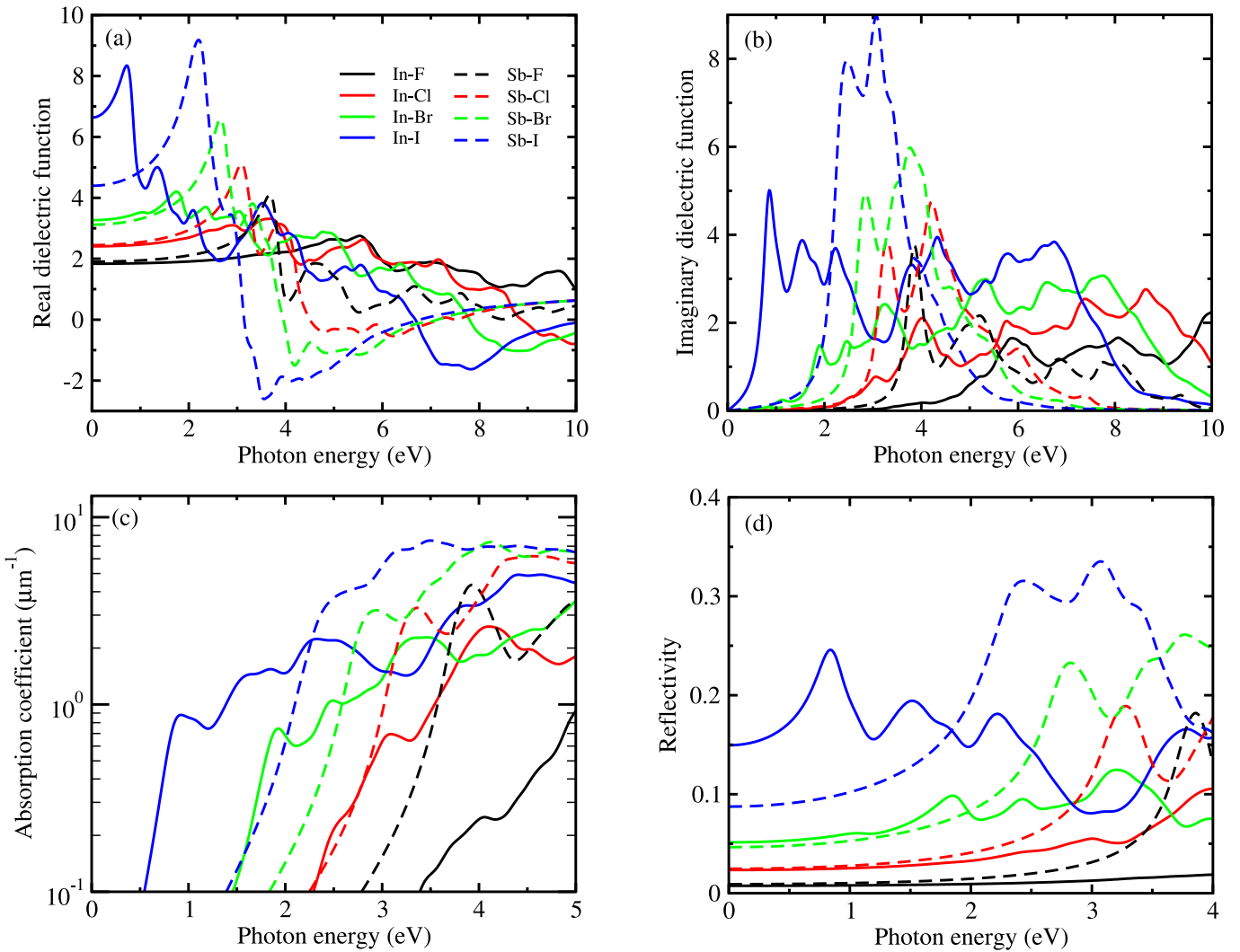


Figure S5. (a) Real and (b) imaginary parts of macroscopic dielectric functions, (c) photo-absorption coefficients, and (d) reflectivity as functions of photon energy for  $\text{Cs}_2\text{AgBX}_6$  ( $B = \text{In}, \text{Sb}; X = \text{F}, \text{Cl}, \text{Br}, \text{I}$ ), calculated with the  $GW$  energies within RPA (i.e.,  $GW$ -RPA).

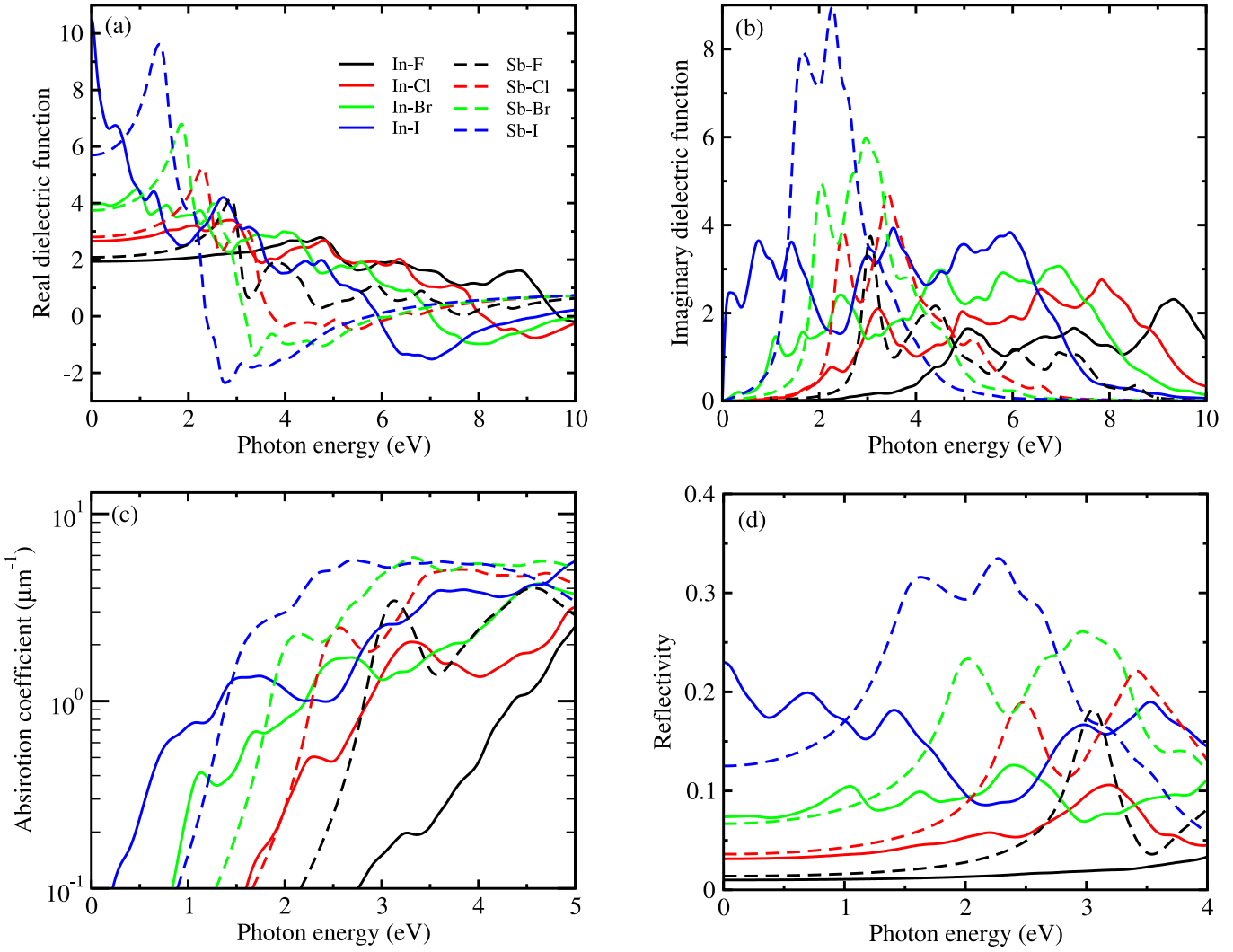


Figure S6. (a) Real and (b) imaginary parts of macroscopic dielectric functions, (c) photo-absorption coefficients, and (d) reflectivity as functions of photon energy for  $\text{Cs}_2\text{AgBX}_6$  ( $B = \text{In}, \text{Sb}; X = \text{F}, \text{Cl}, \text{Br}, \text{I}$ ), calculated with the Kohn-Sham energies within RPA (i.e., KS-RPA).

---

## References

- [1] C. E. Weir, G. J. Piermarini, S. Block, On the crystal structures of Cs II and Ga II, *J. Chem. Phys.* **1971**, *54*, 2768–2770.
- [2] I.-K. Suh, H. Ohta, Y. Waseda, High-temperature thermal expansion of six metallic elements measured by dilatation method and X-ray diffraction, *J. Mater. Sci.* **1988**, *23*, 757–760.
- [3] E. G. Moshopoulou, R. M. Ibberson, J. L. Sarrao, J. D. Thompson, Z. Fisk, Structure of  $\text{Ce}_2\text{RhIn}_8$ : an example of complementary use of high-resolution neutron powder diffraction and reciprocal-space mapping to study complex materials, *Acta Crystal. B* **2006**, *62*, 173–189.
- [4] K. Takemura, H. Fujihaza, High-pressure structural phase transition in indium, *Phys. Rev. B* **1993**, *47*, 8465–8470.
- [5] D. Akhtar, V. D. Vankar, T. C. Goel, K. L. Chopra, Metastable structures of liquid-quenched and vapour-quenched antimony films, *J. Mater. Sci.* **1979**, *14*, 988–994.
- [6] J. Q. Li, X. W. Feng, M. A. Sun, W. Q. Ao, F. S. Liu, Y. Du, Solvothermal synthesis of nano-sized skutterudite  $\text{Co}_{4-x}\text{Fe}_x\text{Sb}_{12}$  powders, *Mater. Chem. Phys.* **2008**, *112*, 57–62.
- [7] S. Hull, D. A. Keen, Pressure-induced phase transitions in  $\text{AgCl}$ ,  $\text{AgBr}$ , and  $\text{AgI}$ , *Phys. Rev. B* **1999**, *59*, 750–761.
- [8] T. Benmessabih, B. Amrani, F. El haj Hassan, F. Hamdache, M. Zoaeter, Computational study of  $\text{AgCl}$  and  $\text{AgBr}$  semiconductors, *Physica B* **2007**, *392*, 309–317.
- [9] B. Amrani, R. Ahmed, F. El haj Hassan, A. H. Reshak, Structural, electronic and optical properties of  $\text{AgI}$  under pressure, *Phys. Lett. A* **2008**, *372*, 2502–2508.
- [10] A. Yoshiasa, K. Koto, K. Kanamaru, S. Emura, H. Horiuchi, Anharmonic thermal vibrations in wurtzite-type  $\text{AgI}$ , *Acta Crystal. B* **1987**, *43*, 434–440.
- [11] P. Cortona, Direct determination of self-consistent total energies and charge densities of solids: A study of the cohesive properties of the alkali halides, *Phys. Rev. B* **1992**, *46*, 2008–2014.
- [12] M. Blackman, I. H. Khan, The polymorphism of thallium and other halides at low temperatures, *Proc. Phys. Soc. London* **1961**, *77*, 471–475.
- [13] C. Hebecker, R. Hoppe, Zur Kristallstruktur von Indium- und Thallium trifluorid, *Naturwissenschaften* **1966**, *53*, 104.
- [14] J. D. Forrester, A. Zalkin, D. H. Templeton, Crystal and Molecular Structure of Indium(III) Iodide ( $\text{In}_2\text{I}_6$ ), *Inorg. Chem.* **1964**, *3*, 63–67.
- [15] A. J. Edwards, Fluoride crystal structures. Part XIV. Antimony trifluoride: A redetermination, *J. Chem. Soc. A* **1970**, *1970*, 2751–2753.